

SAND 90-2254C
12/13/90
Conf 910435-32

BOUNDARY INTEGRAL METHODS FOR UNSATURATED FLOW^a

M. J. MARTINEZ and D. F. McTIGUE
Computational Fluid Dynamics Division
Sandia National Laboratories
Albuquerque, NM 87185
(505) 844-8729

SAND--90-2254C
DE91 005964

DISCLAIMER

This report was prepared as an account of work sponsored by an agency of the United States Government. Neither the United States Government nor any agency thereof, nor any of their employees, makes any warranty, express or implied, or assumes any legal liability or responsibility for the accuracy, completeness, or usefulness of any information, apparatus, product, or process disclosed, or represents that its use would not infringe privately owned rights. Reference herein to any specific commercial product, process, or service by trade name, trademark, manufacturer, or otherwise does not necessarily constitute or imply its endorsement, recommendation, or favoring by the United States Government or any agency thereof. The views and opinions of authors expressed herein do not necessarily state or reflect those of the United States Government or any agency thereof.

MASTER

DISTRIBUTION OF THIS DOCUMENT IS UNLIMITED
[Signature]

ABSTRACT

A boundary integral equation method (BIEM) is described for numerical analysis of quasilinear steady unsaturated flow in homogeneous material. The applicability of the exponential model for the dependence of hydraulic conductivity on pressure head is discussed briefly. This constitutive assumption is at the heart of the quasilinear transformation. Materials which display a wide distribution in pore-size are described reasonably well by the exponential. For materials with a narrow range in pore-size, the exponential is suitable over more limited ranges in pressure head.

The numerical implementation of the BIEM is used to investigate the infiltration from a strip source to a water table. The net infiltration of moisture into a finite-depth layer is well-described by results for a semi-infinite layer if $\alpha D > 4$, where α is the sorptive number and D is the depth to the water table. The distribution of moisture exhibits a similar dependence on αD .

INTRODUCTION

Many large simulations may be required to assess the performance of Yucca Mountain as a possible site for the nation's first high level nuclear waste repository. The governing equations for flow in partially saturated media are, in general, highly nonlinear, and obtaining numerical solutions to some current models may be prohibitively slow and costly. Thus, it is important to explore any approximations and/or new solution methods that offer the potential for greatly improved speed in obtaining solutions, while retaining the critical elements of the transport phenomena. Here we consider steady, multidimensional flows, and adopt a model for hydraulic conductiv-

^aThis work was performed under the auspices of the U.S. Department of Energy, Office of Civilian Radioactive Waste Management, Yucca Mountain project under contract number DE-AC04-76DP00789.

ity in which the conductivity increases exponentially with capillary pressure head. More complex forms for the conductivity may yield better fits to data for some materials, particularly when considering a broad range of capillary pressure head. However, for those problems where the exponential form is an adequate representation of data, the more complex forms offer no significant advantage over the exponential form, while the latter offers potentially large gains in ease of solution. Furthermore, large relative error in estimates of conductivity in dry regions of the problem domain can often be tolerated, since these regions do not participate in the flow. Hence, it is more important for the conductivity model to match data in the moist regions than in the dryer areas.

For the exponential conductivity model, a simple change of dependent variable renders the governing equation linear. This process is referred to as the "quasi-linear transformation," following Philip.¹ The enormous simplification effected by the transformation apparently was first noted by Gardner,² and has since been exploited by numerous workers. Comprehensive reviews of the approach and its application have been presented by Philip^{3,4} and Pullan.⁵ The linear governing equation, of course, permits much simpler and faster solution methods than does the original, nonlinear equation.

In this paper, we explore the boundary integral equation method (BIEM) for obtaining numerical solutions in arbitrary two-dimensional geometries. This scheme, apparently first applied in this context by Pullan and Collins,⁶ offers a number of significant advantages over other, more conventional approaches. The BIEM reduces the dimension of the numerical problem by one in comparison to more conventional domain methods (e.g., finite difference or finite element), typically yielding a much smaller computational problem. Furthermore, the BIEM treats problems in unbounded domains naturally because the fundamental solutions employed satisfy far-field boundary conditions identically. The BIEM yields

fluxes that retain accuracy of the same order as the potential itself because a numerical approximation for the gradient is not required. This is important for radionuclide transport simulations. There are however, several limitations of the present approach which call for further development. Among the most restrictive is that the transformed governing equation is valid only for pressure heads less than or equal to zero; that is, the system of interest must remain unsaturated. In addition the present formulation of the BIEM considers only homogeneous material; the treatment of interfaces between materials of contrasting properties requires further development.

QUASILINEAR ANALYSIS

Steady flow in an unsaturated, rigid, porous medium is described by combining Darcy's law with a statement of mass conservation,

$$\mathbf{q} = -K(\psi)(\nabla\psi - \mathbf{e}_z) , \nabla \cdot \mathbf{q} = 0 , \quad (1)$$

where \mathbf{q} is the fluid flux (volume flow rate per unit area of the medium), K is the hydraulic conductivity (here taken to be isotropic), ψ is the capillary pressure head, and \mathbf{e}_z is the unit vector in the vertical direction (positive downward). The combination of these equations results in the steady form of the Richards equation:

$$\nabla \cdot [K(\psi)(\nabla\psi - \mathbf{e}_z)] = 0 . \quad (2)$$

Because the hydraulic conductivity K is a strongly varying function of ψ , this equation is, in general, highly nonlinear. A model for the hydraulic conductivity that is often used in soil physics is the exponential form,

$$K(\psi) = K_s \exp(\alpha\psi) , \quad -\infty < \psi \leq 0 , \quad (3)$$

where K_s is the conductivity at full saturation and α is a material constant. Clearly, α is simply the slope of a plot of $\ln K$ vs. ψ .

A comparison of the exponential conductivity to the widely used van Genuchten⁷ function, which is a more

general model, was carried out for conductivities believed to be typical of the major tuff units in Yucca Mountain, Nevada. A reasonably good match was obtained for units which show a relatively wide distribution of pore-size. For materials that exhibit a narrow range in pore-size the exponential is suitable over more limited ranges of pressure head. Figure 1 shows a comparison of the exponential and van Genuchten⁷ models for relative permeability ($K(\psi)/K_s$), in which the latter uses currently available material properties representative of Yucca Mountain tuffs.⁸ The range in pressure head shown in Figure 1 was based on calculations from the COVE 2A benchmarking exercise.⁹ These simulations show that for infiltration fluxes of 0.1 mm/yr or greater, pressure heads never fall below -150 m. The Topopah Spring welded unit, which exhibits a wide pore-size distribution relative to the Calico Hills non-vitric unit, can be fit quite well by the exponential. On the other hand, the Calico Hills unit cannot be fit over the full range in pressure head displayed in Figure 1 because of the 'shoulder' in the van Genuchten model, a consequence of a narrow pore-size distribution. However, the corollary to (3),

$$K(\psi) = K_s \exp[\alpha(\psi - \psi_0)], \quad \psi < \psi_0, \quad (4)$$

yields a better match, albeit over a more limited range of pressure head ($\psi_0 = -25$ m in Figure 1b). It is worth noting here that very little data on relative permeability for Yucca Mountain tuffs is available. The parameters for the van Genuchten model used in the comparison with the exponential were not determined by fitting measurements but were developed according to a theory proposed by Mualem¹⁰ and subsequently applied by van Genuchten.⁷ This theory requires data on the moisture retention function only and not on the relative permeability. In the absence of data on relative permeability, there may be no reason to prefer one model over another.

By introducing a Kirchhoff transformation,

$$\Phi = \int_{-\infty}^{\psi} K(\psi) d\psi, \quad (5)$$

the steady Richards equation becomes

$$\nabla^2 \Phi - \alpha \frac{\partial \Phi}{\partial Z} = 0, \quad (6)$$

when the conductivity is exponential in the capillary pressure as defined in (3). The coordinate in the direction of gravity is Z . Furthermore, the Darcy flux becomes

$$\mathbf{q} = -\nabla \Phi + \alpha \Phi \mathbf{e}_z, \quad (7)$$

so that the flux is also a linear function of the potential Φ . Owing to the relation $\alpha \Phi = K(\psi)$, obtained from (4), a contour level of constant potential is also a contour level of constant capillary pressure and moisture content (θ).

BOUNDARY INTEGRAL FORMULATION

Boundary value problems associated with (6) can be reformulated as a boundary integral equation (BIE) through use of Green's second identity. To generate the boundary integral, we use the free-space fundamental solution to (6) in the Green's identity which eventually yields,

$$\begin{aligned} \frac{1}{2} \Phi(\mathbf{x}) + \int_{\Gamma} \frac{\partial G(\mathbf{x}, \mathbf{y})}{\partial n} \Phi(\mathbf{y}) d\Gamma(\mathbf{y}) \\ = \int_{\Gamma} G(\mathbf{x}, \mathbf{y}) [-q_n(\mathbf{y})] d\Gamma, \quad \mathbf{x} \in \Gamma \end{aligned} \quad (8)$$

in which Γ is the bounding surface to the problem domain, Ω , and G is the free-space Green's function satisfying (6) for a point source in an unbounded domain. The normal derivative is defined by $\partial(\cdot)/\partial n = \nabla(\cdot) \cdot \mathbf{n}$, where \mathbf{n} is the outward-pointing unit normal to the boundary, $q_n(\mathbf{y}) = -\partial \Phi / \partial n + \alpha \Phi n_z$ is the flux normal to the boundary surface Γ , and $n_z = \mathbf{n} \cdot \mathbf{e}_z$ is the vertical component of the normal to Γ . This integral equation relates values of the potential and normal flux on the boundary. Interior values of potential are given by a similar equation, obtained by replacing the coefficient 1/2 by unity.

Once the boundary data has been determined, the flux vector in the interior can be computed by operating on (8) (with the 1/2 replaced by unity) according

to (7). Since the gradient operation can be taken under the integral sign, this procedure involves derivatives of the kernels and not of the computed boundary data. For this reason the BIEM yields fluxes of the same order of approximation as the potential itself. More conventional numerical techniques (finite-difference or finite element) require numerical differencing of the potential to obtain fluxes, thereby reducing the accuracy of the latter by one order in mesh size. Pathlines and travel times can also be computed if the retention curve for the material is given.

NUMERICAL TREATMENT

Analytical solution of the BIE is not possible in general; hence, numerical methods are applied. The first step in the numerical approximation of (8) is to discretize the boundary Γ into a number of boundary elements, Γ_n ($n = 1, \dots, N$). In the present version, the boundary elements are all straight line segments. Next, the variations of Φ and q_n over each segment are approximated by their values at the center of the boundary element, hence the numerical approximation to the BIE becomes

$$\frac{1}{2}\Phi(\mathbf{x}_i) + \sum_j \Phi_j G'_{ij} = \sum_j (-q_{nj}) G_{ij} , \quad (9)$$

where $\Phi_j = \Phi(\mathbf{x}_j)$, $q_{nj} = q_n(\mathbf{x}_j)$, and

$$G'_{ij} = \int_{\Gamma_j} \frac{\partial G(\mathbf{x}_i, \mathbf{y})}{\partial n} d\Gamma(\mathbf{y}) ,$$

$$G_{ij} = \int_{\Gamma_j} G(\mathbf{x}_i, \mathbf{y}) d\Gamma(\mathbf{y}) .$$

For purposes of computing the coefficients, it is convenient to describe the geometry parametrically. In the present method we refer the boundary segments to a set of piece-wise linear basis functions, as in the finite element method. The coefficients are then computed with four-point Gauss-Legendre quadrature. The coefficient integrals are improper when the considered point and

boundary element coincide. These coefficients are computed by subtracting the singularity, integrating it analytically and summing with the numerical integral of the remainder.

When we apply the boundary integral equation to each of the N boundary elements, use the boundary conditions (which specify half of the $2N$ point values of potential and flux), and rearrange, we get the linear system $\mathbf{A}\mathbf{u}_h = \mathbf{f}$ where \mathbf{u}_h contains the unknown potential or flux on the boundary and \mathbf{f} contains the inner product of specified boundary values (i.e., boundary conditions) and kernel coefficients. Once the boundary values are determined by solving the linear system by Gaussian elimination, the BIE (8) can be used to compute the potential at any interior point. As noted earlier, the flux vector in the interior can also be computed once the boundary data is determined.

The numerical implementation of the BIE has been tested by comparison with analytical and independent numerical solutions; excellent agreement was found. Convergence studies of the algorithm have shown the rate to be quadratic with uniform boundary element size reduction on smoothly varying solutions. However, this convergence rate is degraded significantly if there are singularities in the problem, for example an abrupt change in boundary condition on the boundary. We find that the quadratic convergence rate can be restored with the mesh grading algorithm suggested by Yan and Sloan.¹¹

INFILTRATION TO A WATER TABLE FROM A STRIP SOURCE

The code written to solve the quasilinear equation has been applied to analyze the infiltration from a strip source of breadth $2L$ to a water table at depth D below the surface. The hydraulic conductivity of these materials was assumed to be described by the exponential model, Equation (3). This problem is prototypical of steady infiltration and the subsurface redistribution of

the moisture as a function of material capillarity. It also illustrates the advantage of the BIEM for half-space problems, which are often a good approximation to the vadose zone in arid regions where the water table may be deep below the surface.

The moisture level is specified on the strip and no-flux conditions are imposed on the remainder of the horizontal surface. In the case of a deep water table, it is assumed that the material approaches a relatively dry condition deep below the surface. This condition is imposed by specifying that the potential vanishes (relative to the source value) far below the surface. Otherwise, the water table is described by specifying saturated conditions at depth D .

Figure 2 shows the distribution of potential $p = \Phi/\Phi_0$, where Φ_0 denotes the specified potential at the source, in the half-space below the surface (deep water table) as a function of the nondimensional sorptive number, $a = \alpha L$. As described earlier, a contour level of potential is also a level of moisture content and relative permeability. The dimensionless sorptive number is a measure of the relative importance of capillary absorption to gravity forces. Small values of a indicate capillary absorption dominates over gravity-driven flow. This is demonstrated in Figure 2, which shows the moisture is broadly spread for $a = 16^{-1}$, and 'finger-like' for $a = 16$. That is, for large a , the moisture introduced at the source falls nearly vertically with small lateral dispersion.

Figure 3 shows the distribution of potential in the layer between the surface and water table for $d = D/L = 20$ and for corresponding values of the nondimensional sorptive number displayed in Figure 2. The role of a is similar in this case to its role for the deep water table. However, the figure also shows that the characteristic capillary fringe thickness above the water table, relative to the layer thickness, is αD ($= ad$). That is, for $ad \gg 1$ the capillary fringe thickness is small relative to D and

the potential distribution deviates from the deep water table results only in a thin boundary layer of thickness $O(\alpha^{-1})$ above the water table. This is evident upon comparing Figures 2 and 3 for $a = 16$. For small ad the capillary fringe is thick (relative to the layer thickness, D) and the potential distributions in the shallow and deep water table regimes are much different. This is illustrated by Figures 2 and 3 for $a = 16^{-1}$.

The net infiltration over the source area is also dependent on the value of ad . Figure 4 shows the net nondimensional infiltration,

$$F_o = \frac{2a}{K_o L} \int_0^L q_z(X, Z = 0) dX$$

as a function of a and d . The infiltration is proportional to a and becomes independent of d for $a > 5$ (in the range of d considered in Figure 4). Furthermore, the infiltration to a finite-depth water table is well-described by results for the semi-infinite layer ($D \rightarrow \infty$) if $\alpha D > 4$.

CONCLUSIONS

A BIEM code has been written for steady, quasilinear flow in two-dimensional domains. The code computes values of potential and/or flux on the domain boundary. The potential and flux can also be computed in the interior, as a postprocessing task, and at any number of arbitrarily placed points. Pathlines and travel times can also be computed if the retention curve for the material is given. The method has been shown to exhibit quadratic convergence with appropriate mesh grading, even on singular problems, and has been tested against both analytical and independent numerical solutions with excellent agreement. Future plans include further study of the applicability of the exponential model for conductivity and development of the capability to include contiguous regions with different material properties.

REFERENCES

1. J. R. PHILIP, "Steady infiltration from buried point sources and spherical cavities," *Water Resources Research*, 4, 1039 (1968).
2. W. R. GARDNER, "Some steady-state solutions of the unsaturated moisture flow equation with application to evaporation from a water table," *Soil Science*, 85, 228 (1958).
3. J. R. PHILIP, "Theory of infiltration," *Advances in Hydroscience*, 5, 215 (1969).
4. J. R. PHILIP, "The scattering analog for infiltration in porous media," *Reviews of Geophysics*, 27, 431 (1989).
5. A. J. PULLAN, "The quasilinear approximation for unsaturated porous media flow," *Water Resources Research*, 26, 1219 (1990).
6. A. J. PULLAN, and I. F. COLLINS, "Two- and three-dimensional steady quasi-linear infiltration from buried and surface sources using boundary element techniques," *Water Resources Research*, 23, 1633 (1987).
7. M. TH. VAN GENUCHTEN, "A closed-form equation for predicting the hydraulic conductivity of unsaturated soils," *Soil Scienc Society of Americal Journal*, 44 892 (1980).
8. E. A. KLAVETTER, and R. R. PETERS, "Estimation of hydrologic properties of an unsaturated fractured rock mass," *Sandia National Laboratories Technical Report*, SAND84-2642, (1986).
9. P. L. HOPKINS, "COVE 2A benchmarking calculations using LLUVIA," *Sandia National Laboratories Technical Report*, SAND88-2511, (1990).

10. Y. MUALEM, "A new model for predicting the hydraulic conductivity of unsaturated porous media," *Water Resources Research*, **12**, 513 (1976).
11. Y. YAN, and I. H. SLOAN, "Mesh grading for integral equations of the first kind with logarithmic kernel," *SIAM Journal of Numerical Analysis*, **26**, 574 (1989).

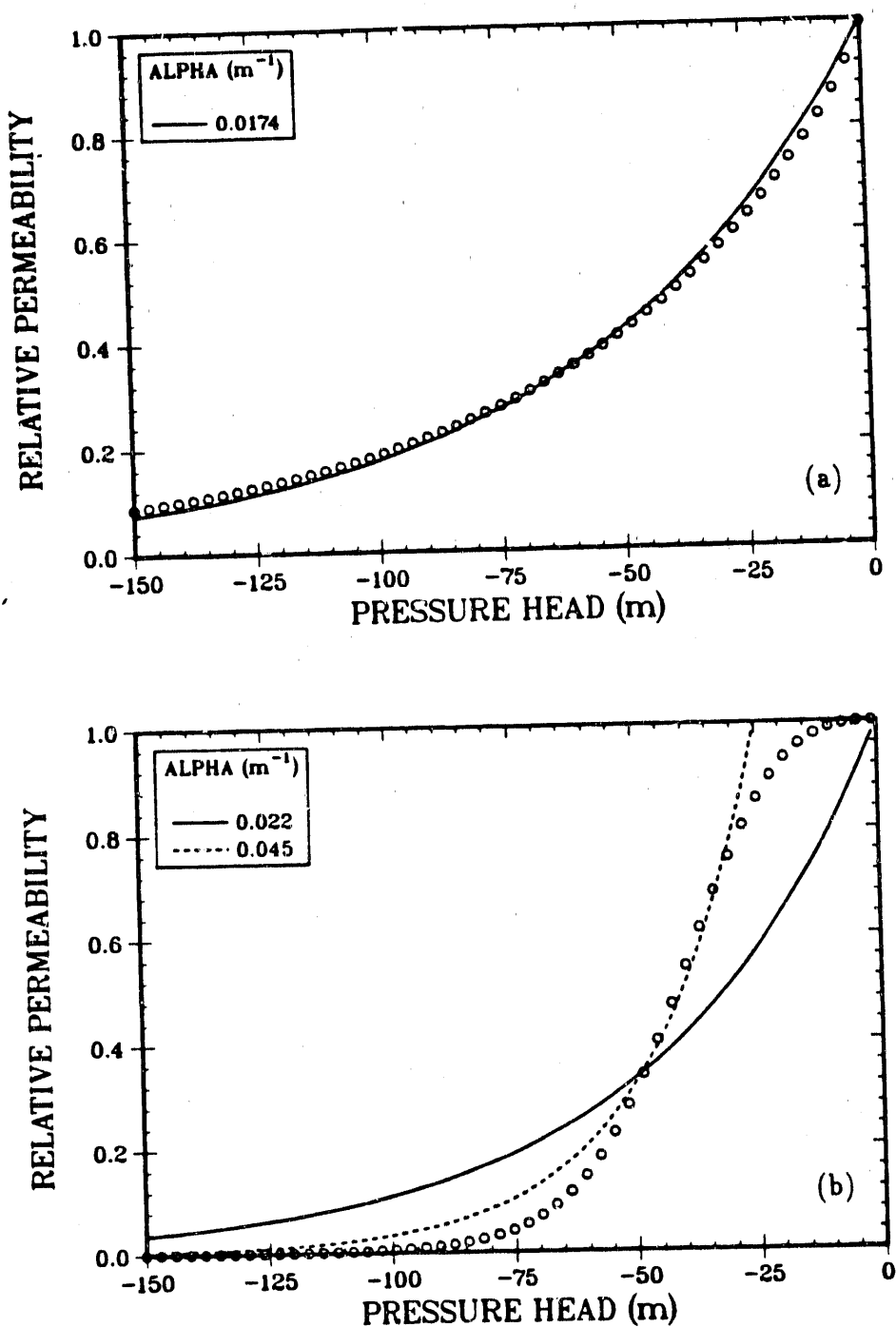


FIGURE 1. Comparison of the van Genuchten (symbols) and exponential (curves) representations of hydraulic conductivity for the (a) Topopah Spring welded unit, and the (b) Calico Hills non-vitric unit. The modified exponential (given by Equation 4 with $\psi_o = -25$ m; dashed line) gives a better match for the Calico Hills, although limiting the range of validity of the exponential.

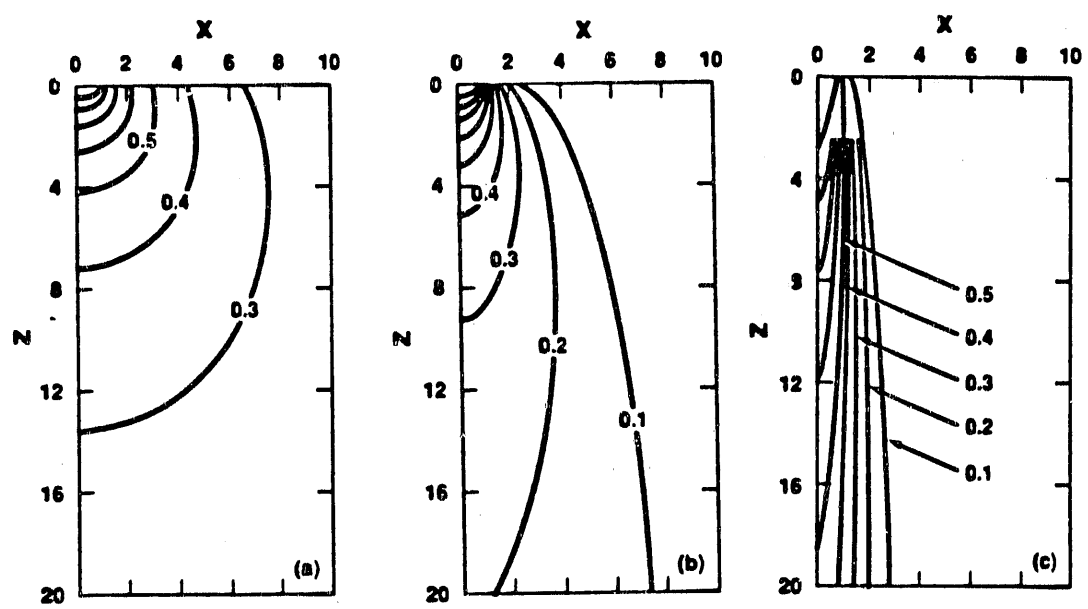


FIGURE 2. Isopotentials for deep water table and (a) $a = 16^{-1}$, (b) $a = 1$, and (c) $a = 16$.

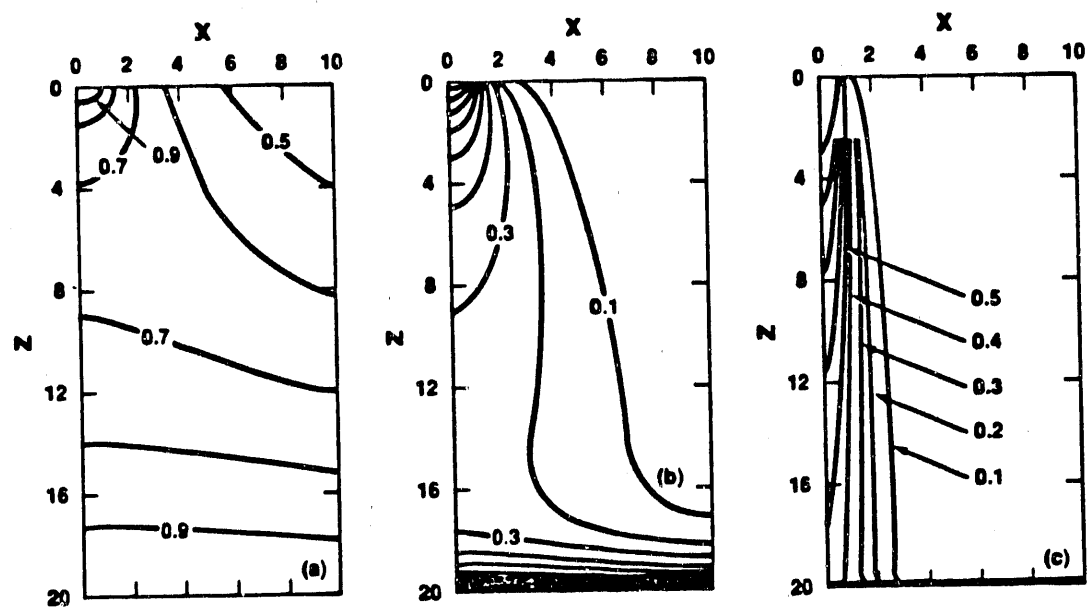


FIGURE 3. Isopotentials for $d = 20$ and (a) $a = 16^{-1}$, (b) $a = 1$, and (c) $a = 16$.

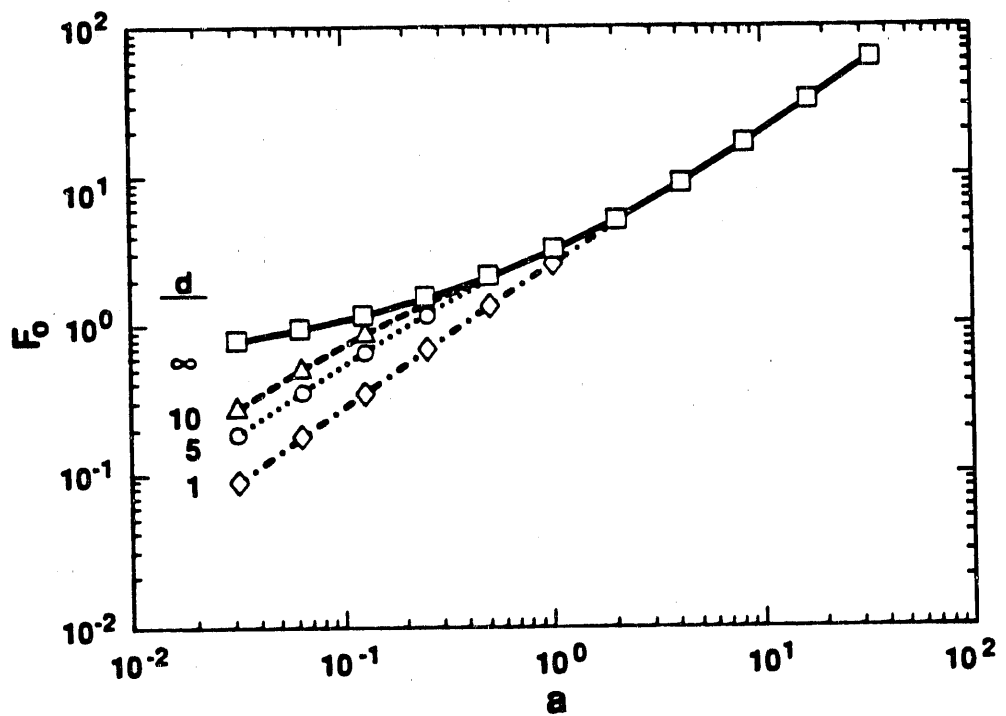


FIGURE 4. Variation of net infiltration through source area with nondimensional sorptive number, $a = \alpha L$, and nondimensional depth to the water table, $d = D/L$.

Sandia National Laboratories
Albuquerque, New Mexico 87185

date: November 12, 1990

to: The reader

MJM

from: M. J. Martinez and D. F. McTigue, 1511

subject: Format for SAND90-2254C

The format for the enclosed manuscript (SAND90-2254C) is temporary; the manuscript will eventually be matted in a double column format.

MJM

END

DATE FILMED

03 / 04 / 91

